ARTICLE

First-Principles Study of $Ca_3Sc_2Si_3O_{12}$:Ce^{3+} Phosphors

Wen Ding[a], Jun Wen[b*], Jun Cheng[a], Li-xin Ning[c], Yu-cheng Huang[c], Chang-kui Duan[a], Min Yin[a]

a. Department of Physics, University of Science and Technology of China, Hefei 230026, China
b. School of Physics and Electronic Engineering, Anqing Normal University, Anqing 246011, China
c. Center for Nano Science and Technology, Department of Physics, Anhui Normal University, Wuhu 241000, China

(Dated: Received on November 2, 2014; Accepted on February 7, 2015)

Charge compensation plays a very important role in modifying the local atomic structure and moreover the spectroscopic property of an isolated luminescent center, and so has been widely adopted in phosphor designs. In this work, we carry out first-principles calculations on various cases of Ce^{3+} centers in $Ca_3Sc_2Si_3O_{12}$ by considering the effects of the charge compensations related to N^{3-}, Sc^{3+}, Mn^{2+}, Mg^{2+}, and Na^{+}. Firstly, the local structures around Ce^{3+} are optimized by using density functional theory calculations with supercell model. The 4f→5d transition energies of Ce^{3+} are then obtained from the CASSCF/CASPT2/RASSI-SO calculations performed on Ce^{3+}-centered embedded clusters. The calculated energies support the previous assignments of the experimental spectra. Especially, a previously unclear peak is identified to be caused by Sc^{3+} substituting Si^{4+}. The results show that the first-principles calculations can be used as an effective tool for predicting and interpreting spectroscopic properties of the phosphors.

Key words: $Ca_3Sc_2Si_3O_{12}$:Ce^{3+}, 4f→5d transition, First-principles, Charge compensation, Excitation spectra

I. INTRODUCTION

Cerium-doped inorganic compounds have attracted much attention because of their wide applications in scintillators, lasers, and phosphors for white light-emitting diodes (w-LEDs) [1, 2]. w-LEDs are regarded as a promising lighting source in the future. Currently, the most widely used w-LEDs consist of yellow-emitting $Y_3Al_5O_{12}$:Ce^{3+} (YAG:Ce^{3+}) phosphors and blue InGaN LEDs [3−5]. However, YAG:Ce^{3+} emits little red light, which does not meet the requirement of warm-white LED. Full-color-emitting single-phase phosphors are thus expected. Many studies have been devoted to the development of high performance phosphors of red as well as other colors [6−9]. Thereinto, $Ca_3Sc_2Si_3O_{12}$:Ce^{3+} (CSS:Ce^{3+}) attracts a lot of attention due to its high intensity and high thermal stability. It is known, from the X-ray absorption fine structure analysis, that Ce^{3+} ions occupy Ca^{2+} sites with many types of possible charge compensation mechanisms [9−13]. The local atomic structures of Ce^{3+} can be modified by the charge compensation ions, which would affect the 5d states, and moreover, the 5d→4f luminescence of Ce^{3+}. The emission colors of the phosphors are thus tuned. Some tentative assignments of the peaks in the optical spectra of CSS:Ce^{3+} to certain type of charge compensation mechanisms have been made [10−13].

In this work, we carry out first-principles calculations [14, 15] to investigate the effects of different types of charge compensation mechanisms on the structural and spectroscopic properties of CSS:Ce^{3+} phosphors. In previous experiments [10−13], some of the peaks in the excitation spectra of CSS:Ce^{3+} are not identified. We compare the calculated 4f→5d transition energies with the excitation spectra to make some detailed assignments and analyses. The feasibility and accuracy of the first-principles calculations is demonstrated, an effective and convenient method of investigating luminescent properties of Ce-doped phosphors is provided.

II. METHODOLOGY

Ce-doped CSS crystal is modeled by means of a 2×2×2 supercell containing 160 atoms, in which one of the 24 Ca atoms is substituted by a Ce atom. For each supercell, the geometry optimization is carried out with density functional theory (DFT) [16, 17] calculations within the generalized gradient approximation (GGA), using the Vienna *ab initio* Simulation Package [18, 19]. The $3p^64s^2$ electrons on Ca, the $3d^14s^2$ electrons on Sc, the $2s^22p^4$ electrons on O, the $3s^23p^2$ electrons on Si, and the $5s^25p^64f^15d^16s^2$ electrons on Ce are treated as valence electrons, and their interactions with the respective cores are described by the projected augmented wave method [20]. The geometry op-

*Author to whom correspondence should be addressed. E-mail: wenjunkd@mail.ustc.edu.cn

 ©2015 Chinese Physical Society

TABLE I Calculated and measured lattice parameters for pure and doped CSS from which we construct embedded clusters.

CSS	$2a$/Å	$2b$/Å	$2c$/Å	Volume/Å^3	Embedded clusters
Pure, expt.[35]	12.250	12.250	12.250	1838.27	
Pure, calc.	12.338	12.338	12.338	1878.05	
Ce^{3+}	12.356	12.356	12.356	1886.41	$(CeO_8Si_2)^{5-}$
Ce^{3+}, N^{3-}	12.376	12.375	12.366	1894.13	$(CeNO_7Si_2)^{6-}$
Ce^{3+}, Mg^{2+}	12.355	12.365	12.359	1888.15	$(CeO_8Si_2Mg)^{3-}$
Ce^{3+}, Mn^{2+}	12.345	12.362	12.363	1887.91	$(CeO_8Si_2Mn)^{3-}$
Ce^{3+}, Na^{+}	12.356	12.356	12.357	1887.37	$(CeO_8Si_2)^{5-*}$
Ce^{3+}, Sc^{3+}	12.381	12.427	12.379	1904.63	$(CeO_8SiSc)^{6-}$

* For Ce^{3+}, Na^{+} co-doped CSS crystal, the Na^{+} ion (3.766 Å away from the Ce^{3+} center) locates in the immediate lattice environments around the embedded cluster $(CeO_8Si_2)^{3-}$ rather than in it.

timizations are performed by using the conjugate gradient technique, until the total energies are converged to 1 μeV and the Hellmann-Feynman forces on the atoms are less than 0.01 eV/Å. We used a plane-wave cutoff energy of 550 eV with one k-point Γ for sampling the Brillouin zone.

The Ce-centered embedded clusters are constructed on the basis of the Perdew-Burke-Ernzerhof (PBE) optimized [21] geometries of the supercells, on which the wave function-based *ab initio* calculations are performed to obtain the 4f and 5d energies. For the Ce-centered embedded clusters, consisting of the central Ce^{3+} ions and their coordinating anions, with 350−360 surrounding ions within a sphere of a 10.0 Å radius modeled using the *ab initio* model potential (AIMP) to account for the short-range electrostatic, exchange, and Pauli interactions of the clusters with their environments; the rest of ions located within a sphere of radius 30.0 Å are regarded as point charges. For the embedded clusters, the state-average SA-CASSCF [22−25] plus CASPT2 [26−28] calculations are performed with a scalar relativistic many-electron Hamiltonian, with considering the bonding, static and dynamic correlation effects. The AMFI approximation of the DKH spin-orbit coupling operator [29−31] is added to the Hamiltonian with the CASSCF wave functions and the CASPT2 energies, and a restricted active space state-interaction spin-orbit (RASSI-SO) method [32] is used to include the spin-orbit coupling effect. These wave function-based calculations are performed by using the program MOLCAS [33]. In the SA-CASSCF calculations, a [4f, 5d, 6s] complete active space is adopted. The CASSCF wave functions come from interactions of all configurations in which the single unpaired electron occupies one of the 13 molecular orbitals of main characters Ce^{3+} 4f, 5d, and 6s. The molecular orbitals are optimized by minimizing the average energy of the 13 states. CASPT2 calculations are carried out, where dynamic correlation effects of the Ce^{3+} 5s, 5p, 4f, and 5d electrons and the O^{2-} 2s and 2p electrons are considered with the CASSCF wave functions and the occupied and virtual orbitals.

III. RESULTS AND DISCUSSION

CSS:Ce^{3+} is a novel emission-tunable silicate garnet phosphor, in which Ca, Sc, and Si cations being eight-, six-, and four-coordinated in dodecahedron, octahedron, and tetrahedron, respectively. The doping Ce^{3+} are supposed to occupy Ca^{2+} sites, due to the matched ionic radii (1.12 and 0.745 Å for eight-coordinated Ca^{2+} and six-coordinated Sc^{3+}, respectively, and 1.143 and 1.01 Å for eight- and six-coordinated Ce^{3+}, respectively) [34]. Firstly, the structural optimization calculation is implemented on the pure CSS. In Table I, it can be found that the calculated value of the lattice constant (a=b=c) is 12.338 Å, slightly larger than the experimental value of 12.250 Å, as generally expected for the GGA-PBE calculations. The four Ca−O bond lengths in pure CSS are calculated to be 2.411 Å, another four as 2.551 Å, and thus are in good agreement with the experimentally measured ones (2.390 and 2.532 Å, respectively) [35]. The effects of a series of impurity ions on the structural properties of CSS:Ce^{3+} are then verified, which are demonstrated in Fig.1. One can see that the dopant induces distortion of the local atomic structures around Ce^{3+}, and also slightly changes the volumes of the supercell.

First, we consider the case without charge compensation in the local coordination environment of Ce^{3+}, which means that the co-doped N^{3-} (adopted herein) has a long distance (9.40 Å) away from the luminescence center. The calculated Ce−O bond lengths are slightly larger than the counterparts in pure CSS, due to the matched ionic radii for Ce^{3+} and Ca^{2+}. When N^{3-} is doped into the local environment of Ce^{3+} to occupy one of the nearest neighboring O^{2-} site, the optimized bond length of Ce−N is smaller than that of the corresponding Ce−O for Ce^{3+} without a neighboring N^{3-}, while the other Ce−O bond lengths increase. The contraction of Ce−N bond length can be ascribed to the stronger electrostatic interaction between Ce^{3+} and

DOI:10.1063/1674-0068/28/cjcp1411190 ©2015 Chinese Physical Society

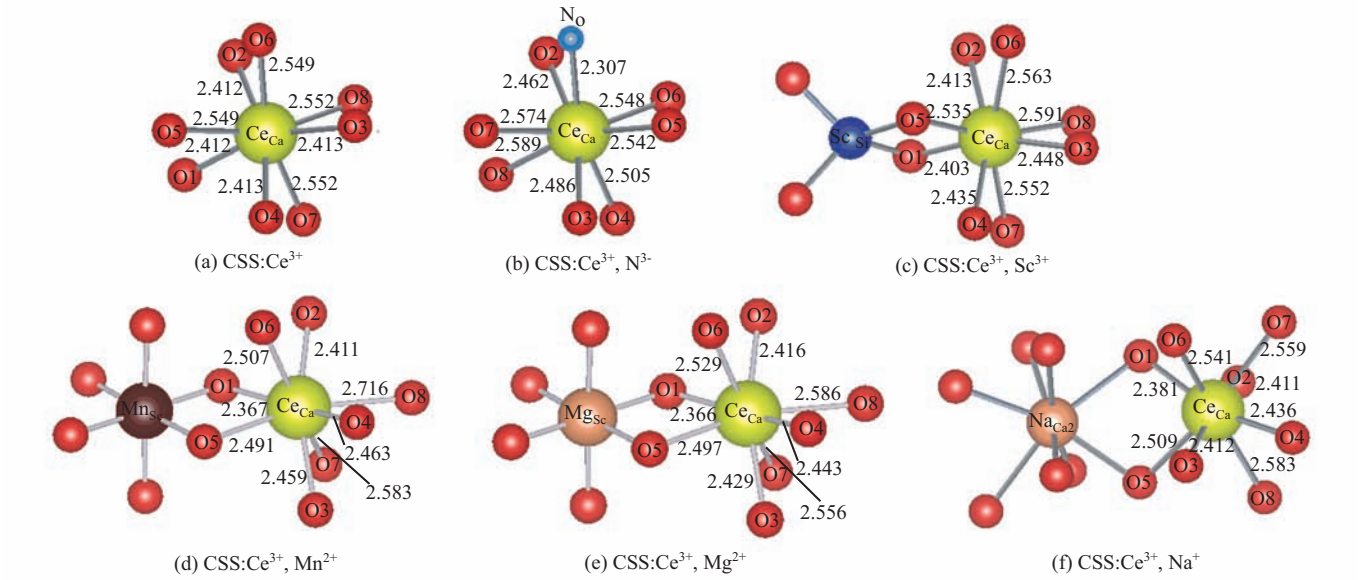

FIG. 1 DFT optimized local atomic structures around Ce^{3+} in CSS with different types of charge compensation mechanisms.

TABLE II Calculated and measured energies of $4f^1$ and $5d^1$ levels of Ce^{3+} doped in $Ca_3Sc_2Si_3O_{12}$.

CSS	Ce^{3+}		Ce^{3+}, N^{3-}		Ce^{3+}, Sc^{3+}		Ce^{3+}, Mn^{2+}	Ce^{3+}, Mg^{2+}	Ce^{3+}, Na^{+}
	Calc.	Expt.[12]	Calc.	Expt.[11]	Calc.	Expt.[10]	Calc.	Calc.	Calc.
$4f^1$	0		0		0		0	0	0
	337		546		556		745	358	314
	751		1106		932		1085	830	708
	2269		2200		2221		2212	2241	2231
	2331		2549		2542		2808	2338	2323
	2681		3168		2987		3156	2885	2712
	2319		4129		4165		4044	3844	3714
$5d^1$	22922	22222	20699	19960	21988		22892	22754	23109
	31972	32580	30922		30403	29851	31773	32143	31818
	45594		41634		42826		45007	45383	45070
	49874		45081		48610		48248	48745	49228
	51040		52034		51531		52290	51440	50882

N^{3-} ions, which meanwhile leads to the change of the other Ce−O bond lengths. When Mn^{2+} or Mg^{2+} substitutes a Sc^{3+} site near the dopant Ce^{3+}, the lengths of four or three of the Ce−O bonds become shorter, while the rest four or five bond lengths become longer.

Based on the DFT-optimized crystal structures, we construct Ce-centered embedded clusters (Table I) for 4f and 5d crystal-field level calculations [36], *i.e.* with their surroundings represented by AIMPs and point charges at the lattice sites. The energy levels of $4f^1$ and $5d^1$ configurations of Ce^{3+} in CSS are obtained from the CASSCF/CASPT2/RASSI-SO calculations on the chosen embedded clusters including $(CeO_8Si_2)^{5-}$, $(CeNO_7Si_2)^{6-}$, $(CeO_8SiSc)^{6-}$, $(CeO_8Si_2Mn)^{3-}$, $(CeO_8Si_2Mg)^{3-}$, and $(CeO_8Si_2)^{5-}$. The crystal-field parameters (CFPs) of Ce^{3+} with different local environments are extracted [36] from the *ab initio* calculated energy levels and wave functions. On the basis of the calculated 4f and 5d CFPs, the 4f→5d absorption spectra (see Fig.2) are thus simulated to achieve the straightforward comparison with the experimental spectra. In Table II, we show the calculated energy levels, along with the available experimental spectroscopic data. One can see that the calculated $5d_{1,2}$ energy levels for the Ce^{3+} without other co-doping ions in its local environment agree well with the experimental excitation bands of the two lowest 4f→5d transitions of Ce^{3+} (*i.e.*, the $Ce^{3+}(1)$ sites in the Ref.[11]), and the largest deviation between the calculated and experimental 5d energy levels is less than 800 cm^{-1}. This shows the accuracy of the adopted first-principles calculations at the CASSCF/CASPT2/RASSI-SO level.

DOI:10.1063/1674-0068/28/cjcp1411190 ©2015 Chinese Physical Society

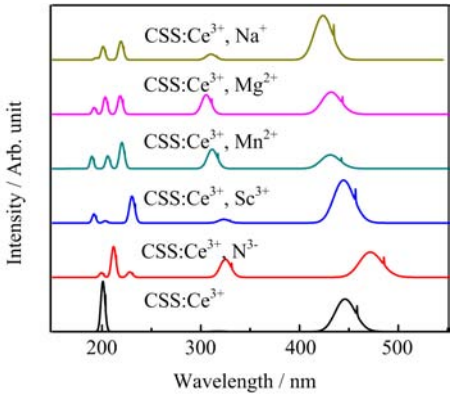

FIG. 2 Simulated absorption spectra for Ce^{3+} in CSS with different types of charge compensation mechanisms.

For the Ce^{3+} with N^{3-} in its local environment, the 5d energy levels obviously decrease (in the range of 1000 cm^{-1} to 4000 cm^{-1}) except the highest one, which increases around 1000 cm^{-1}. We attribute it to the stronger crystal field felt by Ce^{3+} due to the shorter distance between Ce^{3+} and N^{3-}. According to Ref.[11], there are two intense peaks at ∼510 and ∼450 nm in the excitation spectrum [11] of Ce^{3+}, N^{3-} co-doped CSS phosphor. It can be found that the calculated $5d_1$ energy level is in good agreement with the first peak at ∼510 nm. Moreover, the second peak agrees well with the calculated $5d_1$ energy level of the Ce^{3+} without N^{3-} in its local environment. Hence, our calculations show the strong proof of the analysis of the experimental literatures that two types of Ce^{3+} sites exist in Ce^{3+}, N^{3-} co-doped CSS, *i.e.*, Ce^{3+} with and without N^{3-} in its local environment.

For the charge compensation mechanisms related to Mn^{2+}, Mg^{2+}, and Na^{+}, the calculated results show that the effect of these impurity ions on the energy-level structure of Ce^{3+} is small. It should be noted that Mn^{2+} ions can occupy both Ca^{2+} and Sc^{3+} sites in CSS to act as the luminescence centers, and emit yellow and red lights, respectively. Furthermore, the substitution of Si^{4+} by Sc^{3+} in the local environment of Ce^{3+} can also be the possible charge compensation mechanism [11]. It is noted that the $5d_2$ energy level of Ce^{3+} (*i.e.*, 30403 cm^{-1}) matches the second peak in the excitation spectra (see Ref.[13]). Hence, our calculations indicate that the peak at around 340 nm in the excitation spectra can be attributed to the second 4f→5d transition of the Ce^{3+} with Sc^{3+} substituting Si^{4+} in its local environment, which was unidentified before.

IV. CONCLUSION

We carried out structure optimization calculations for CSS:Ce^{3+} with various charge compensation mechanisms, and then derived the 4f→5d transition energies of Ce^{3+} from the CASSCF/CASPT2/RASSI-SO calculations. The calculated transition energies are in good agreement with the peaks in the measured excitation spectra for the corresponding charge compensation cases. Especially, our calculations confirm that the two excitation peaks in the excitation spectra of $Ca_3Sc_2Si_3O_{12}$:Ce^{3+}, N^{3-} (at about 510 and 450 nm, respectively) are ascribed to the two types of Ce^{3+}, *i.e.*, with and without a N^{3-} in their local coordination environments. Furthermore, a previously unclear excitation peak at around 340 nm is now identified to be from the 4f→$5d_2$ transition of Ce^{3+} with a near Si^{4+} substituted by Sc^{3+}.

V. ACKNOWLEDGMENTS

This work was supported by the National Key Basic Research Program of China (No.2013CB921800), the National Natural Science Foundation of China (No.11374291, No.11311120047, No.11274299, No.11447197, and No.11204292), the Fundamental Research Funds for the Central Universities (No.WK20304200), the Anhui Provincial Natural Science Foundation (No.1508085QA09). The numerical calculations have been partially done on the supercomputing system in the Supercomputing Center of University of Science and Technology of China.

[1] E. F. Schubert and J. K. Kim, Science **308**, 1274 (2005).
[2] X. L. Dong, J. H. Zhang, X. Zhang, Z. D. Hao, and Y. S. Luo, J. Lumin. **148**, 60 (2014).
[3] J. Oliva, E. De la Rosa, L. A Diaz-Torres, A. Torres, P. Salas, and O. Meza, J. Lumin. **154**, 185 (2014).
[4] S. Nakamura, S. J. Pearton, and G. Fasol, *The Blue Laser Diode*: *The Complete Story*, New York: Springer-Verlag, 230 (2000).
[5] K. Bando, K. Sakano, Y. Noguchi, and Y. Shimizu, J. Light Visual Environ. **22**, 2 (1998).
[6] Y. Q. Li, J. E. J. van Steen, J. W. H. van Krevel, G. Botty, A. C. A. Delsing, F. J. DiSalvo, G. de With, and H. T. Hintzen, J. Alloys Compd. **417**, 273 (2006).
[7] K. Uheda, N. Hirosaki, Y. Yamamoto, A. Naito, T. Nakajima, and H. Yamamoto, Electrochem. Solid-State Lett. **9**, H22 (2006).
[8] A. A. Setlur, W. J. Heward, Y. Gao, A. M. Srivastava, R. G. Chandran, and M. V. Shankar, Chem. Mater. **18**, 3314 (2006).
[9] Y. Shimomura, T. Honma, M. Shigeiwa, T. Akai, K. Okamoto, and N. Kijima, J. Electrochem. Soc. **154**, J35 (2007).
[10] J. Qiao, J. H. Zhang, X. Zhang, Z. D. Hao, Y. F. Liu, and Y. H. Luo, Dalton Trans. **43**, 4146 (2014).
[11] J. Qiao, J. H. Zhang, X. Zhang, Z. D. Hao, W. Y. Deng, Y. F. Liu, L. L. Zhang, L. G. Zhang, H. F. Zhao, and J. Lin, Opt. Lett. **38**, 6 (2013).
[12] Y. F. Liu, X. Zhang, Z. D. Hao, X. J. Wang, and J. H. Zhang, Chem. Commun. **47**, 10677 (2011).

DOI:10.1063/1674-0068/28/cjcp1411190 ©2015 Chinese Physical Society

[13] Y. Shimomura, T. Kurushima, M. Shigeiwa, and N. Kijima, J. Electrochem. Soc. **155**, J45 (2008).
[14] L. X. Ning, C. B. Wu, L. L. Li, L. H. Lin, C. K. Duan, Y. F. Zhang, and L. Seijo, J. Phys. Chem. C **116**, 18419 (2012).
[15] J. Wen, L. X. Ning, C. K. Duan, Y. H. Chen, Y. F. Zhang, and M. Yin, J. Phys. Chem. C **116**, 20513 (2012).
[16] P. Hohenberg and W. Kohn, Phys. Rev. **136**, B864 (1964).
[17] W. Kohn and Sham, L. Phys. Rev. **140**, A1133 (1965).
[18] G. Kresse and J. Furthmülle, Phys. Rev. B **54**, 11169 (1996).
[19] G. Kresse and D. Joubert, Phys. Rev. B **59**, 1758 (1999).
[20] P. E. Blöch, Phys. Rev. B **50**, 17953 (1994).
[21] P. Perdew, K. Burke, and M. Ernzerhof, Phys. Rev. Lett. **77**, 3865 (1996).
[22] B. O. Roos, P. R. Taylor, and P. E. M. Siegbahn, Chem. Phys. **48**, 157 (1980).
[23] P. E. M. Siegbahn, A. Heiberg, B. O. Roos, and B. Levy, Phys. Scr. **21**, 323 (1980).
[24] P. E. M. Siegbahn, A. Heiberg, J. Almlöf, and B. O. Roos, J. Chem. Phys. **74**, 2384 (1981).
[25] K. Andersson, P. Å. Malmqvist, B. O. Roos, A. J. Sadlej, and K. Wolinski, J. Phys. Chem. **74**, 5483 (1990).
[26] K. Andersson, P. Å. Malmqvist, and B. O. Roos, J. Chem. Phys. **74**, 1218 (1992).
[27] A. Zaitsevskii and J. P. Malrieu, Chem. Phys. Lett. **74**, 597 (1995).
[28] J. Finley, P. Å. Malmqvist, B. O. Roos, and L. Serrano-Andrés, Chem. Phys. Lett. **288**, 299 (1998).
[29] M. Douglas and N. M. Kroll, Ann. Phys. **82**, 89 (1974).
[30] B. A. Hess, Phys. Rev. A **33**, 3742 (1986).
[31] B. A. Hess, C. Marian, U. Wahlgren, and O. Gropen, Chem. Phys. Lett. **251**, 365 (1996).
[32] P. Å. Malmqvist, B. O. Roos, and B. Schimmelpfennig, Chem. Phys. Lett. **357**, 230 (2002).
[33] G. Karlstöm, R. Lindh, P. Å. Malmqvist, B. O. Roos, U. Ryde, V. Veryazov, P. O. Widmark, M. Cossi, B. Schimmelpfennig, P. Neogrady, and L. Seijo, Comput. Mater. Sci. **28**, 222 (2003).
[34] R. D. Shannon, Acta Crystallogr. **A32**, 751 (1976).
[35] B. V. Mill, E. L. Belokoneva, M. A. Simonov, and N. V. Belov, Zhurnal Strukturnoi Khimii. **18**, 399 (1977).
[36] J. Wen, C. K. Duan, L. X. Ning, Y. C. Huang, S. B. Zhan, J. Zhang, and M. Yin, J. Phys. Chem. A **118**, 4988 (2014).

DOI:10.1063/1674-0068/28/cjcp1411190 ©2015 Chinese Physical Society